frontiers | Frontiers in Built Environment

TYPE Original Research
PUBLISHED 05 December 2023
DOI 10.3389/fbuil.2023.1301126

OPEN ACCESS

EDITED BY
Martin Koller,
University of Graz, Austria

REVIEWED BY
Wenbo Ma,
Xiangtan University, China
Elisabete Fraga Freitas,
University of Minho, Portugal

*CORRESPONDENCE
Hao Liang,
lianghao@sdjtky.cn

RECEIVED 24 September 2023
ACCEPTED 24 November 2023
PUBLISHED 05 December 2023

CITATION
Fan J, Liang H, Sun Z and Chen Z (2023), Investigation on strength characteristics and mechanism of cold mix based on geopolymerization reaction.
Front. Built Environ. 9:1301126.
doi: 10.3389/fbuil.2023.1301126

Investigation on strength characteristics and mechanism of cold mix based on geopolymerization reaction

Junying Fan[1], Hao Liang[2]*, Zhiping Sun[1] and Zhao Chen[3]

[1]Shandong Hi-speed Construction Management Group Co., Ltd., Jinan, China, [2]Shandong Transportation Institute, Jinan, China, [3]Shandong Expressway Peninsula Investment Co., Ltd., Jinan, China

Cold mix asphalt is an energy-efficient and eco-friendly pavement material, yet its early strength is deficient. This study investigated the strength augment of cold mix asphalt through modification with geopolymer additives. Macro-strength was assessed via Marshall stability testing under varied geopolymer contents, curing durations, and water immersion conditions. Microscale analysis encompassed fluorescence microscopy to discern geopolymer-asphalt interactions and discrete element modeling to simulate the compression process. Results showed that stability rose and then fell as geopolymer content increased, with an optimal ratio of 4:3 between base asphalt and additive. Stability increased rapidly in the first 3 days of curing and accumulated at a slower rate afterwards. Fluorescence microscopy revealed that geopolymer bonded the asphalt to the aggregate surfaces. Modeling exhibited geopolymer resisted vertical loads and confined the aggregate. In summation, geopolymerization enhances cold mix strength by improving adhesion and generating a rigid 3D network encompassing aggregate particles. The discoveries provide guidance on formulating durable cold mix asphalt utilizing geopolymer additives.

KEYWORDS

geopolymer, cold-mix asphalt mixtures, stability, fluorescence microscopy, discrete element modeling

1 Introduction

With the deepening of green construction philosophies, cold mixture technologies are gaining popularity in conventional asphalt pavement construction and maintenance. This technology eliminates the need for high-temperature mineral and asphalt paving, leading to a significant reduction in construction energy consumption and gas emissions, which is a pinnacle of the industry's novel technical innovations (Wang, 2018; Deb and Singh, 2022). However, owing to the deficient initial stability of cold asphalt mixture (hereafter referred to as cold mix), its application in road structures is confined to the lower layers of the pavement and cannot directly function as a surface; alternatively, it can only serve as the rural roads with low traffic demand (Wielinski et al., 2019), which restricts the technology's diffusion. To this end, numerous investigators have conducted studies aimed at improving the sturdiness, adhesion, durability and other attributes of cold mix. For instance, academics have utilized waterborne epoxy resin to modify emulsified asphalt as cold mix asphalt, which can prodigiously enhance high temperature and water stability (Bi et al., 2020; Cai et al., 2020). Incorporating polyurethane into rock asphalt to prepare cold mix asphalt can intensify strength and low temperature crack resistance (Yang, 2019). Some scholars

have utilized inexpensive inorganic materials like cement and lime, blending them into emulsified asphalt cold mixes, which can effectively enhance stability and decrease expenditures (Yang et al., 2014; Meocci et al., 2017; Dulaimi et al., 2023). Similarly, researchers have tried various approaches to boost the performance of cold mix asphalt. Deb and Singh. (2022) and Mondal et al. (2023) enhanced properties like strength, moisture resistance, and rutting resistance by utilizing industrial wastes like steel slag, copper slag, and waste glass as a sustainable solution. According to Guo et al. (2023), rejuvenators made from waste oils, bio-oils, or petroleum-based oils have been shown to soften the aged binder and improve the performance, thereby addressing aging issues in cold mix. The incorporation of nano-materials including nano-silica, nano-titanium dioxide, and nano-copper oxide has been exhibited to improve both the microstructure and performance of cold mix asphalt, as elucidated by Mirabdolazimi et al. (2021) and Mostafa (2015), owing to the enhanced dispersion and adhesion caused by these nanoscale constituents, which lead to intensified stability. Reviews from Alnadish et al. (2023) and Perca et al. (2019) have shown that the inclusion of fibers such as polyester, cellulose, mineral wool can enhance tensile strength and prevent cracking by increasing toughness. Andrews et al. (2023) optimized mix design factors like emulsion content, mineral filler ratio, and aggregate gradation to boost moisture resistance. These emerging solutions use sustainable materials, nano-technology, and optimized design to enhance the properties of cold mix asphalt and expand its competitive applicability. With ongoing advancements in cold mix modification techniques, its prospects for widespread adoption in high-quality pavements are promising, but additional improvement of critical performance factors is obligatory to extend its usage to superior roads. Conceiving sustainable modifying additives and optimized mix configurations will be instrumental in refining the competitiveness of cold mix asphalt in the future.

Geopolymerization is an inorganic chemical reaction process that occurs without heating, wherein the strength formation of the material system is expeditious, and the durability intensifies with prolonged curing ages, as elucidated by Wang et al. (2019). Specifically, geopolymers are formed by the reaction of aluminosilicate source materials with alkaline activators, yielding an amorphous three-dimensional alumino-silicate binder network, as described by Provis et al. (2006) and Duxson et al. (2007). The geopolymerization process involves the dissolution of Si and Al atoms from the source materials, followed by reorientation into oligomers under alkaline conditions, and further polycondensation between oligomers to form the rigid binder structure, as explained by Jindal et al. (2023). The high alkalinity triggers the geopolymerization reactions and allows synthesis of these inorganic polymers at ambient temperatures, enabling the novel cold mix asphalt application proposed in this study. Given the current state of practice, this paper leverages the geopolymerization principles by utilizing inorganic materials and diluent asphalt to develop and evaluate cold mixed asphalt concrete. By taking geopolymers as additives, cold mix based on geopolymerization fundamentals was conceived, with testing and analysis undertaken on strength performance and water stability aspects to ascertain optimal geopolymer dosages and suitable curing periods for this cold mix. Additionally, through microscopic observation and discrete element microscopic simulation trials, the strength characteristics and microscopic compressive mechanism of cold mix were investigated.

The remainder of this paper is structured as follows: Section 2 presents the preparation of materials and design of the cold mixed asphalt; Section 3 conducts macroscopic performance evaluation and analysis of the cold mix modified with geopolymers; Section 4 explores the microstructure and microscopic strengthening mechanism through advanced characterization; and finally, Section 5 summarizes the conclusions and prospects for future research directions.

2 Materials and methods

2.1 Material composition and preparation

2.1.1 Diluted asphalt

The diluted asphalt utilized a solvent-based cold mix asphalt that is relatively easy to produce and economical in price. The diluent employed in this paper was kerosene and Shell 70# asphalt was selected as the matrix asphalt, with pertinent indices depicted in Table 1, fulfilling the requirements of the Technical Specifications for Construction of Highway Asphalt Pavements (JTG F40-2004) (hereafter referred to as Specifications) (Ministry of Transport of the People's Republic of China, 2004).

This study prepared cold mix asphalt by blending additive, asphalt, and diluent at specified mass ratios. The preparation procedure was as follows: First, 70 # asphalt was added to a stirrer pot at a ratio of 1.8:100 and heated to 150°C for 2 h to induce flowability. Next, the additive was introduced to the asphalt at 200 rpm for 10 min to ensure thorough mixing and homogeneity. The additive utilized in this work was manufactured by Beijing Jiagewy Road Construction Technology Co., Ltd and consisted of a multifunctional polymer modifier capable of enhancing the adhesion, aging resistance, and waterproofing of the asphalt. Finally, the diluent was incorporated into the asphalt colloid at a ratio of 25:100, followed by continued stirring at 100 rpm for 30 min, allowing the even dispersion of the diluent throughout the asphalt colloid. Upon completion of mixing, the cold mix asphalt was prepared.

2.1.2 Geopolymer

The geopolymer additives constituted the formulated geopolymers, principally encompassing sodium silicate (in liquid form), sodium hydroxide (NaOH) inorganic alkali, and other substances. The sodium silicate was produced by a certain chemical company in Jiaxing City, with the chemical composition and physical parameters delineated in Table 2.

The NaOH was manufactured by a chemical reagent company in Tianjin, possessing a relative molecular mass of 40.00 and maximum mass fraction of impurities of 3.4%. In this study, the geopolymer activator was prepared by mixing sodium silicate and NaOH at a mass ratio of 1:1. The mixture was stirred until the solution regained transparency, then left to stand at room temperature. Separately, a certain amount of mineral powder was added to a stirrer pot and dispersed evenly. The configured alkaline activator was poured into the pot at a water-to-solid ratio of 2, followed by rapid stirring for 10 min and then slow stirring for 5 min until the materials in the pot

TABLE 1 Technical indexes of 70# matrix asphalt.

Test item	Penetration (25°C,5s,100 g)/(0.1 mm)	Ductility (10°C,5 cm·min^{-1})/cm	Softening point ($T_{R\&B}$)/°C	Flash point/°C
Standard	60–80	≥20	≥46	≥260
Test	72	35	47.5	336

TABLE 2 Chemical composition and physical parameters of sodium silicate.

Composition and attribute	Mass fraction/%			Density/(g·cm^{-3})	Modulus
	SiO_2	Na_2O	H_2O		
Numerical value	29.9	13.75	56.35	1.48	2.25

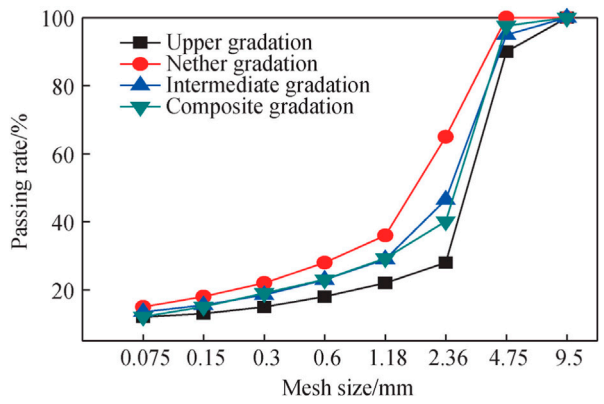

FIGURE 1
Design grading curves.

were gelatinized. The homogenized slurry was taken out for later use.

2.1.3 Aggregates and gradation

The aggregates utilized limestone from Jinan, Shandong Province, with the mineral powder and associated indices fulfilling the Specifications requirements. To optimize the formation of gelation products between the geopolymer and mineral powder within the aggregates (Wang et al., 2020), the SMA-5 gradation was selected as the mix design type for the cold mix asphalt, which has smaller particle sizes, greater contact surface area, and stable structure. The grading curve is depicted in Figure 1.

In alignment with the Specifications and engineering experience, the mass ratio of asphalt to aggregate (asphalt refers to the total amount of base asphalt and additives) was prescribed as 7%. To avoid compromising the cold mix cohesion by excessive mineral powder, the dosage was limited to 3%–5% of the total aggregate mass, and the aggregate quantities were adjusted reasonably to ensure a dense skeleton structure (Zhang, 2007).

2.1.4 Preparation of cold mix

The cold mix asphalt was blended using an asphalt concrete mixer, following these steps: first, the aggregates and dilute asphalt were mixed evenly, then the geopolymer and mineral powder were added and blended further. To ensure uniform blending, the cold mix components were heated at different temperatures according to the Specifications and repeated blending experiments, as shown in Table 3.

Since the geopolymers are inorganic, a defined curing period is necessitated for post specimen molding to develop strength. In alignment with the curing cycles stipulated in the Test Code of Inorganic Cementitious Stabilizing Materials for Highway Engineering (JTG E51-2009) and the intrinsic properties of the geopolymers, sealed curing at room temperature for 7 days was selected as the curing condition.

2.2 Methods

The gelation substances generated by the geopolymers can effectively enhance the compressive strength of cold mix asphalt (Hamid et al., 2020). However, excessive gelation may impede contact between some asphalt and aggregates, compromising the cold mix cohesion. To optimally elucidate the impact of geopolymer additives on cold mix strength, this study implemented the Marshall stability test as a macro-scale experimental technique, utilizing stability assessment indices to evaluate the strength and stability performance of the cold mix. The Marshall test is extensively utilized to evaluate the stability and flow properties of asphalt mixtures. Its standardized testing procedure and simple operation make it a prevalent approach for assessing the performance of cold mix asphalt. Although the Marshall test cannot fully simulate the working conditions under traffic loading, the stability index can effectively reflect the compressive strength and overall structural stability trend of the mixture, which is highly consistent with the present study as a preliminary investigation into the mechanical performance and stability of cold mixed asphalt. Meanwhile, the standardized experimental methodology minimizes variability in the test execution, thus helping ensure repeatability and reliability of the data acquisition.

Cylindrical Marshall specimens of dimensions 101.6 mm × 63.5 mm were immersed in a 60°C water bath for 0.5 h, then loaded at 50 mm/min using a Marshall stability apparatus, as depicted in Figure 2.

To verify the water stability, the immersion Marshall test was conducted, whereby specimens were cured for 48 h under defined

TABLE 3 Heating temperatures of different components.

Components	Aggregate	Cold mix asphalt	Mineral powder	Geopolymer additive
Temperature/°C	60	80	25(Normal)	25(Normal)

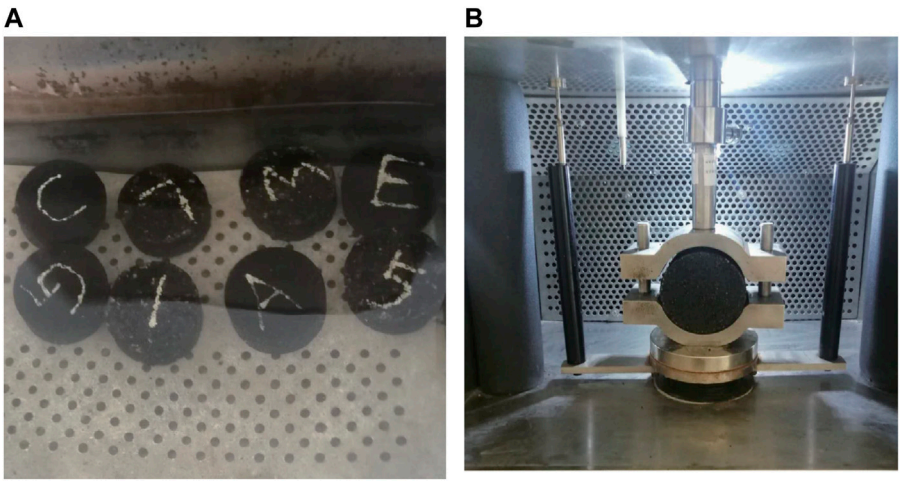

FIGURE 2
(A) Specimens immersed in water at constant temperature; **(B)** Loading process of specimen.

immersion temperature prior to testing, with the residual stability index computed per formula (1), evaluating the strength and water stability under immersed conditions.

$$M_{S0} = \frac{M_{S1}}{M_S} \times 100 \quad (1)$$

Where M_{S0} is the residual stability, %; M_S is the stability; M_{S1} is the stability after immersion in water for 48 h.

To probe the strength characteristics and microscopic mechanism of the geopolymer additives, fluorescence microscopy and discrete element analysis were applied. Fluorescence microscopy enables direct observation of the microstructure in the cold mixed asphalt, clearly presenting the interfacial bonding between the geopolymer, asphalt, and aggregates. Meanwhile, discrete element simulation establishes a virtual model on the computer to simulate the loading damage process of the Marshall test, assessing the internal mechanical responses of the mixture (Xiao et al., 2021; Yao et al., 2022). The two techniques are complementary to each other, with one directly characterizing the microscopic morphology and the other simulating the microscopic mechanisms, jointly revealing the strengthening mechanism of the geopolymer modification.

3 Macroscopic performance evaluation

3.1 Effect of geopolymer additive dosage on strength

In this study, geopolymer additive dosages were increased gradually to elucidate the impacts, with the mass ratios of matrix asphalt to geopolymer additives set at 4:0, 4:1, 4:2, 4:3, 4:4, 4:5, and 4:6 for analysis. The resulting stability test data is portrayed in Table 4.

TABLE 4 Stability of cold mix under different geopolymer additive dosage.

Proportion	4:0	4:1	4:2	4:3	4:4	4:5	4:6
Stability	6.88	7.67	8.31	9.12	8.14	6.98	6.27
Standard	≥3						

It is discerned from Table 4 that the stability initially escalates then diminishes with increasing geopolymer dosage, reaching a maximum at 4:3, and dropping markedly below average when the ratio is 4:6. Upon initial incorporation of the geopolymers, the geopolymerization reaction yielded a certain quantity of gelation products, which could envelop and bond the aggregate surfaces, thereby enhancing the overall structural strength of the mixture. This accounts for the early-stage intensification of strength. However, as the geopolymer dosage continued to rise, excessive gelation products were generated. The superfluous gelation began to accumulate and aggregate, with its volumetric effect impeding the efficient adhesive contact area between asphalt and aggregates. Concurrently, some gelation may have absorbed asphalt components originally intended for bonding. This led to a decline in the cohesive interactions between asphalt and aggregates, consequently attenuating the stability of the mixture, which explains the later stage declines in strength. Overall, while the initial geopolymerization boosted cohesion, the excessive quantities obstructed bonding resulting in debilitated strength. The optimized dosage represents the equilibrium between both effects, simultaneously enhancing the geopolymer strengthening while preventing adhesion loss.

TABLE 5 Immersion results of cold mix under different geopolymer additive dosage and temperatures.

Proportion		4:0	4:1	4:2	4:3	4:4	4:5	4:6
60°C	stability/kN	6.88	7.63	8.27	9.06	8.11	6.98	6.24
	immersion stability/kN	2.01	1.89	1.65	1.75	1.02	—	—
	residual stability/%	29.22	24.64	19.68	19.19	12.53	0.00	0.00
25°C	stability/kN	6.95	7.93	8.85	10.14	9.23	8.82	8.52
	immersion stability/kN	6.23	6.91	7.67	8.63	7.54	7.05	6.11
	residual stability/%	89.64	87.14	86.67	85.11	81.69	79.93	71.71
Standard/%		≥85						

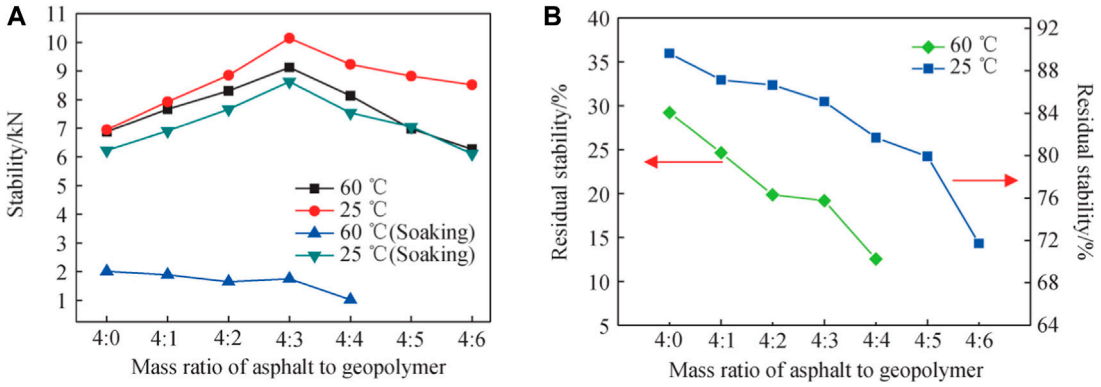

FIGURE 3
(A) Stability of cold mix under different geopolymer additive content and temperatures; **(B)** Residual stability of cold mix under different geopolymer additive content and temperatures.

3.2 Effect of water immersion on strength

Further analysis was undertaken utilizing the water immersion Marshall test. With a ratio reaching 4:5, the specimens exhibited a semi-loose state subsequent to immersion at 60°C, attributable to the reduced asphalt content and excessive softening after high temperature exposure compromising cohesion. Therefore, stability testing proceeded on specimens immersed for 48 h at 25°C, with residual stability computed to obtain the experimental results under varied geopolymer dosages, as delineated in Table 5.

The compiled stability and residual stability curves of the cold mix at diverse geopolymer contents and temperatures are depicted in Figure 3. Figure 3A demonstrates the stabilities at 25°C uniformly exceeded those at 60°C, indicating temperature as the predominant factor impacting strength, while geopolymer incorporation did not effectively mitigate its influence. The drastically reduced stability from 25°C to 60°C highlights the sensitivity of the cold mix strength to temperature exposure. However, under identical conditions, the stability trends followed consistent maxima at 4:3 for all dosages. Per Figure 3B, with increasing geopolymer, the residual stability gradually declined at both temperatures, partly owing to the reduced asphalt quantity weakening cohesion, and partly the relatively feeble water damage resistance of the geopolymers. The water immersion testing highlights the vulnerability of this cold mix to high temperatures, the optimal geopolymer ratio for strength, as well as the adverse effects of excessive geopolymer content and inherent water sensitivity.

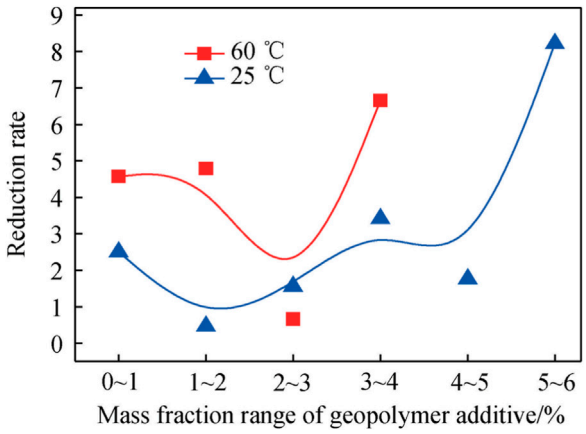

FIGURE 4
Reduction rate of residual stability of geopolymer additive in each interval.

TABLE 6 Stability under different curing time.

Curing time/d	0	3	7	10	14
Stability/kN	2.81	6.92	9.52	10.48	10.92

The reduction rate of residual stability was calculated by finding the slope between adjacent points at two different temperatures, as indicated in formula (2).

$$v = \frac{m_{si} - m_{si-1}}{d_i - d_{i-1}} \quad (2)$$

Where v is the reduction rate of residual stability; d_i is the position of point i on the x-axis; m_{si} is the residual stability at point i. Figure 4 shows the reduction rate and fitting curve of the residual stability of geopolymer additives in each interval.

Analysis of the reduction rate v revealed a decrement followed by an increment trend. Within the geopolymer additive mass fraction interval of 1%–2% and 2%–3%, the residual stability loss reached its lowest point, and in the same proportional range, the v at 60°C was generally higher than that at 25°C, intimating that higher temperature exacerbates the deleterious effects of water and expedites the declination of strength of the cold mix. In the range of 2%–3%, the deviation between v at the two temperatures attained its nadir, signifying that the cold mix exhibited optimal stability within this range, with minimal deleterious effects from water and the slowest reduction rate of strength at disparate temperatures. Consequently, this cold mix manifested the most diminished temperature sensitivity.

3.3 Effect of curing time on strength

As cold mix asphalt pavement pertains to the surface layer, traffic should be opened expeditiously without prolonged curing. Therefore, this study stipulated the maximal curing duration as 14 days in a routine indoor sealed ambiance, with the inception of curing timed following the completion of the molded specimens. Stability tests were enacted on specimens at curing durations of 0 days, 3 days, 7 days, 10 days, and 14 days, incorporating with the optimal blending ratio of 4:3 between the matrix asphalt and geopolymer additive introduced in Section 2.2.

As shown in Table 6, at 0 days curing, the newly formed geopolymer engendered inferior strength with stability beneath specifications. However, post 3 days, stability incrementally accreted. To further elucidate the evolution of strength with age, the growth rate at disparate curing durations were analyzed per formula (3).

$$S = \frac{m_{s2} - m_{s1}}{D_2 - D_1} \quad (3)$$

Where S is the growth rate; M_s is the stability; D is curing time. The increase in intensity and growth rate are shown in Figure 5.

As shown in Figure 5A, the overall stability increased with longer curing duration, which aligns with the geopolymerization reaction needing time to develop strength. However, the accretion of strength declined progressively with prolonged curing. From 10 to 14 days, stability only increased by 0.44 kN, with a mean growth rate of merely 0.15 kN/day. This diminishing strength growth rate can be explained by the geopolymerization reaction slowing down over time. In the early stage around 3–7 days, the dissolution of Si and Al atoms and rapid polycondensation between oligomers contributed to a fast increase in strength. But as the geopolymer network formed, the remaining unreacted fly ash and alkali gradually decreased, thereby limiting the reaction rate.

In Figure 5B, although overall specimen strength increased with curing duration from the incipient time, the strength growth rate still waned. In the initial 3 days of curing, a markedly steep linear slope is discerned, intimating fast strength accretion likely attributable to the relatively high reaction kinetics in this duration. However, beyond 7 days, the slope exhibits a downward trend, signifying attenuated strength accretion rates resulting from depletion of reactive substrates as the geopolymerization neared completion. In summary, extended curing consistently increased stability but the marginal improvements diminished, particularly beyond 10 days. Balancing strength gain *versus* construction timing, the curing period should be at least 3 days to meet the strength specifications.

4 Microstructure and microscopic strengthening mechanism

4.1 Microstructure

Fluorescence microscopy was utilized to scrutinize the cold mix with geopolymer additive, as delineated in Figures 6, 7. It was discerned that the gelated substance engendered by the geopolymer additives cooperated with the asphalt to constitute an adhesive layer affixed to the aggregate surface, also adhering some tiny aggregate particles. Given the sequence where the geopolymer was incorporated after the preliminary blending of the asphalt and aggregates in the cold mix, the gelated material was inclined to accumulate enswathe the exterior surfaces of the aggregates and asphalt. Consequently, when external forces are imposed during service loading, the geopolymer-rich exterior interphase sustains the initial loading as the primary stress receptor. Similarly, upon damage evolution, microcracking is prone to originate within the geopolymer-enriched exterior, as corroborated by the following simulated discrete element modelling. The geopolymer additives created a better interfacial transition zone, which boosted the adhesion and resisted the applied stresses on the composite. However, its external location also exposed it to vulnerability as the primary target of damage.

4.2 Discrete element microscopic analysis

Based on discrete element theory, this study established a two-dimensional discrete element model of the Marshall specimen for cold mixed asphalt concrete using PFC^{2D}. Considering the relatively fine aggregates with indistinct angularities in SMA-5, ball units of different sizes were directly generated to substitute aggregates of various particle sizes, in order to reduce servo operation time and achieve efficient simulation.

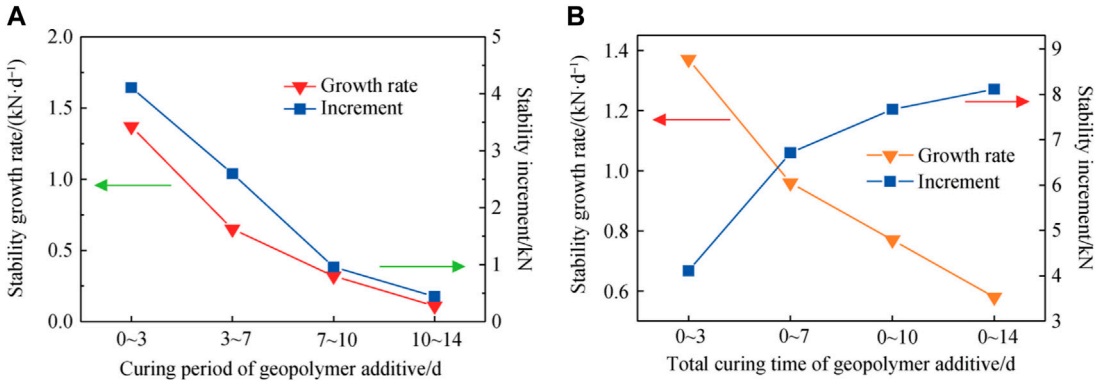

FIGURE 5
(A) Change of stability growth in different curing periods; **(B)** Change of stability growth with curing time.

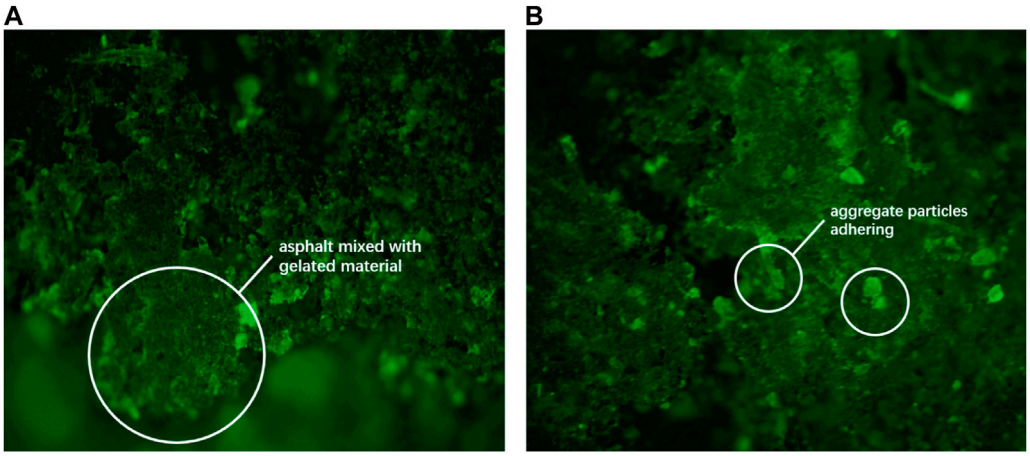

FIGURE 6
(A) Fluorescence micrograph with the magnification of 10; **(B)** Fine aggregate particles attached to the surface (x10).

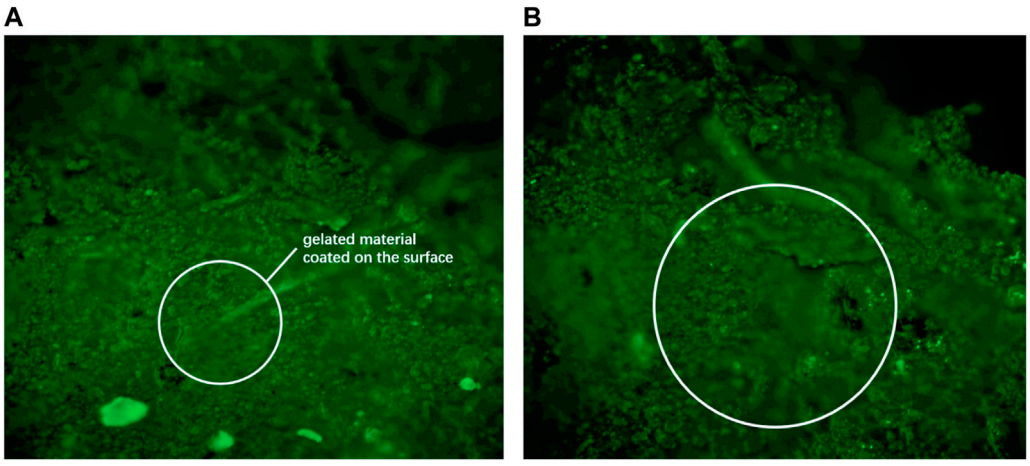

FIGURE 7
(A) Fluorescence micrograph with the magnification of 20; **(B)** Mutual adhesion between binder and asphalt (x20).

TABLE 7 Gradation and composition ratio of SMA-5 cold mix asphalt mixture.

Component	Aggregate			Asphalt in cold mix		Additive
	3~5 mm	0~3 mm	Mineral powder	Matrix asphalt	Diluent	Geopolymer
Volume fraction/%	66	30	4	4	1	3

TABLE 8 Parameters of point contact model.

Point bonding parameter	kn/(N·m^{-1})	ks/(N·m^{-1})	fric
Parameter setting	1×10^{8}	1×10^{8}	0.25

Given the partial 0–3 mm aggregates could integrate with the asphalt and geopolymer additives to constitute the corresponding mortar, this paper follows the Fuller curve and the observed compacted bulk density, and chooses a suitable virtual molding gradation percentage by integrating laboratory trials and theoretical analysis (Olsson et al., 2019), as shown in Table 7, to ensure that the model faithfully reflects the composition percentage and structural attributes of cold mixtures.

The contact model between coarse aggregate particles was further established as point contact, implying that there was only one contact point between particles, and the contact force was propagated along the contact normal direction. The associated parameters of the contact model are displayed in Table 8.

The asphalt mortar and geopolymer were represented by 0.6–1.18 mm circular particles. Since the cold mix with geopolymer additive did not fulfill viscoelastic traits, parallel bonding models were instituted to simulate the bonding between mixtures, with parameters referenced from relevant literature (Liu and You, 2011) as adduced in Table 9.

After establishing the geometric and mechanical models for the asphalt mixture, the boundary constraints and loading plates in the split tensile test were represented by two rigid walls, respectively. During the loading process, to ensure the discrete element model was close to static equilibrium and approximate the split test conditions in the lab, the upper wall was assigned a downward loading velocity of 50 mm/s, while the lower wall remained fixed. The simulation cycles were terminated upon the instantaneous load declining to 70% of its peak value, thereby enabling FISH language programming to output the cracking damage in the asphalt mixture during the computational procedure.

Figure 8 reveals the simulated Marshall specimen loading damage process, where the large particles denote 3–5 mm aggregates, medium particles are 0–3 mm aggregates, and the gelated geopolymer-asphalt are small particles. It can be seen that the failure cracks were discerned directly below the loading point upon damage.

Figure 9 exhibits the variation trend of the contact force distribution from the initial state to the damaged state. It can be observed that with increasing loading, the contact forces also gradually intensified and were predominantly concentrated below the loading point vertically. This indicates the vertical orientation under the loading point endured the maximal contact forces as the primary bearing area. After damage, the contact forces were absent at the cracks, signifying failure occurred in the region sustaining the greatest forces, thus validating the vertical location below the loading point as vulnerable location in terms of brittle fracture.

Figure 10A exhibits the tension and compression force distribution nephogram during specimen damage, evincing indicating internal compression and external tension, with fissures engendered by excessive pressures. The distribution pattern indicates the complex stress states inside the specimen under compression. The exterior tension and interior compression imply structural instability and incipient damage. The fissures verify failure initialization at the locations of maximum compression stress concentration. Figure 10B illustrates the ruptured bond fractures upon specimen damage, with dissevered bonds discernible at the cracks. The discontinuity of bond forces directly reflects the loss of integrity and load transfer capacity. The maximum compressive strength was attained at these fissures, corresponding to the crest stresses in the curve in Figure 11. The full stress-strain response exhibits the typical ascending trend before peak strength, followed by a decrease with reduced stiffness after the peak. The simulated curve shape and key points are highly consistent with the actual experimental measurements. This validation supports the feasibility and reliability of utilizing discrete element modeling and simulations to characterize the mechanical performance and compressive damage processes of cold mix asphalt specimens in stability tests.

Since the displacement morphology of aggregates during compressive loading directly reflects the salient microscopic variations, simulations analyzing the aggregate displacements were conducted. Figure 12 reveals the particle displacement nephogram during compressive loading.

Initially, the specimen was in a stable compression stage with relatively static particle displacements. This indicates the particles were under elastic deformation without overall structural disturbance. As the pressure progressively intensified, instability in the displacement directions transpired internally, with tendencies for contrary motion against the pressure, constituting internal vortex forces. The non-uniform and disorganized displacements imply stress redistribution and incipient structural instability. With further escalating pressures exceeding the specimen strength,

TABLE 9 Parallel bonding parameters.

Parallel bond parameter	kn/(N·m^{-1})	ks/(N·m^{-1})	fric	Band gap/mm	Pb_ten/Pa	Pb_coh/Pa	dp_nratio
Parameter setting	1×10^{8}	1×10^{8}	0.25	0.5 × 10^{-4}	2×10^{7}	5×10^{7}	0.5

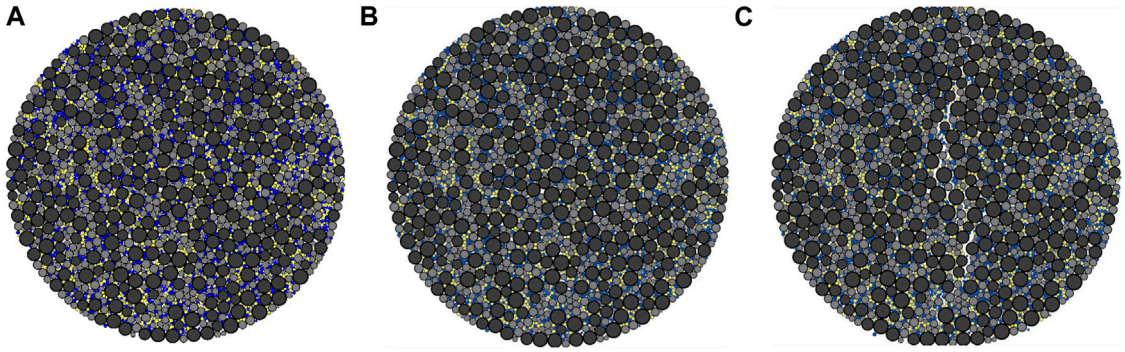

FIGURE 8
Damage process of virtual Marshall specimen during loading. **(A)** Initial; **(B)** Loading; **(C)** Damage.

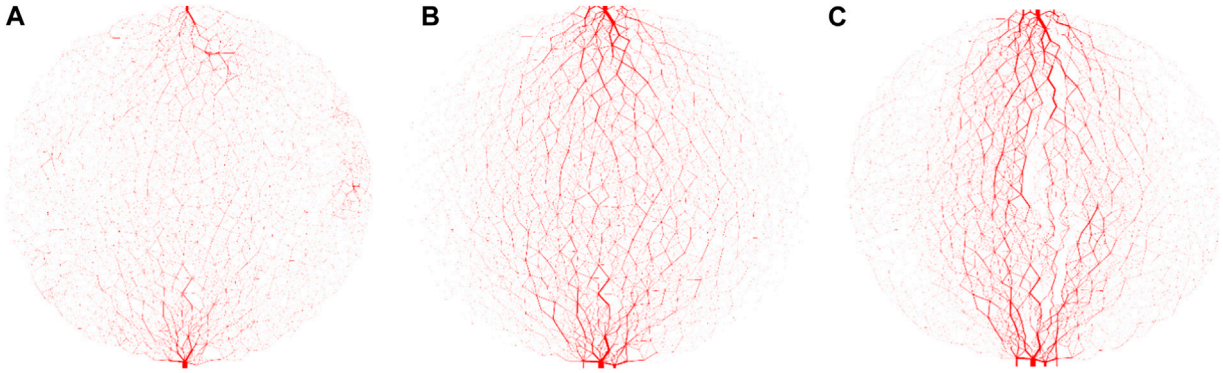

FIGURE 9
Contact force distribution during loading. **(A)** Initial; **(B)** Loading; **(C)** Damage.

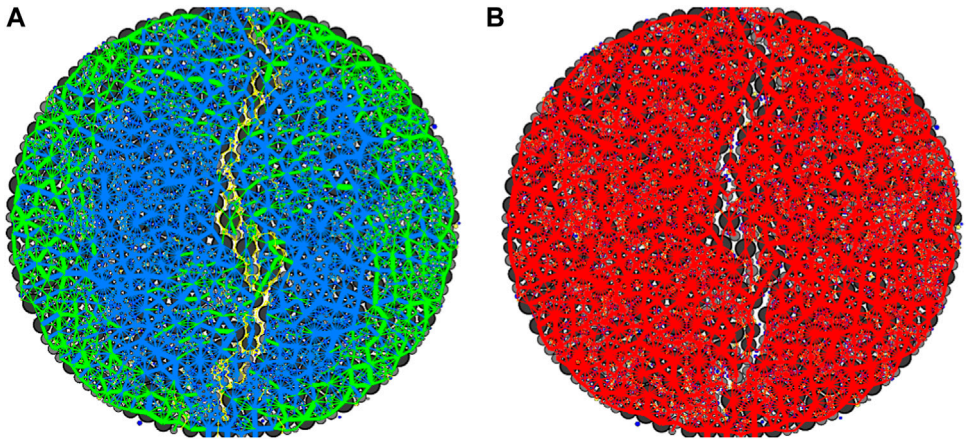

FIGURE 10
(A) Tensile (outside) and compression (inside) positions of specimen after damage; **(B)** Fracture of bond.

particles began shifting from the centre outwards. The collective lateral movements of particles demonstrate the specimen was no longer able to sustain homogeneous compression, leading to stress concentration and failure initialization. Eventually, rupture occurred at the vertical loading point, further evidencing this as the predominant compressive force orientation. The displacement

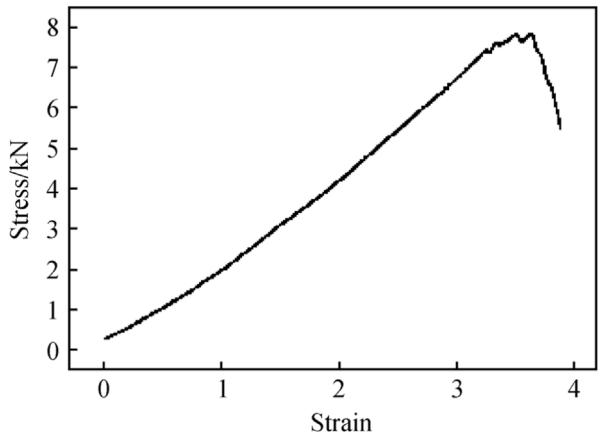

FIGURE 11
Stress-strain curve under virtual test.

evolution and propagation of failure verify the loading point as the weakest point.

In summation, during the Marshall test, the vertical orientation below the loading point endures the principal loading. Loading resistance and deformation capacity are largely determined by the vertical strength and stiffness. In the cold mix, asphalt alone as the binder enhances the bonding strength, but falls short of the strength attained by the gelated geopolymer envelopment after sufficient curing. The rigid geopolymer network provides confinement and loading transfer between aggregates. Therefore, based on the foregoing analysis, in the absence of factors like water damage, the addition of certain geopolymer additives can substantially enhance the strength of the cold mix asphalt. This simulated result aligns with the findings in the previous part of this paper, indicating the geopolymer additives is the primary factor impacting cold mix strength, and also the main contributor to the enhanced strength. Meanwhile, the simulation supplements and deepens the conclusions of the exposed previously, revealing the microscale

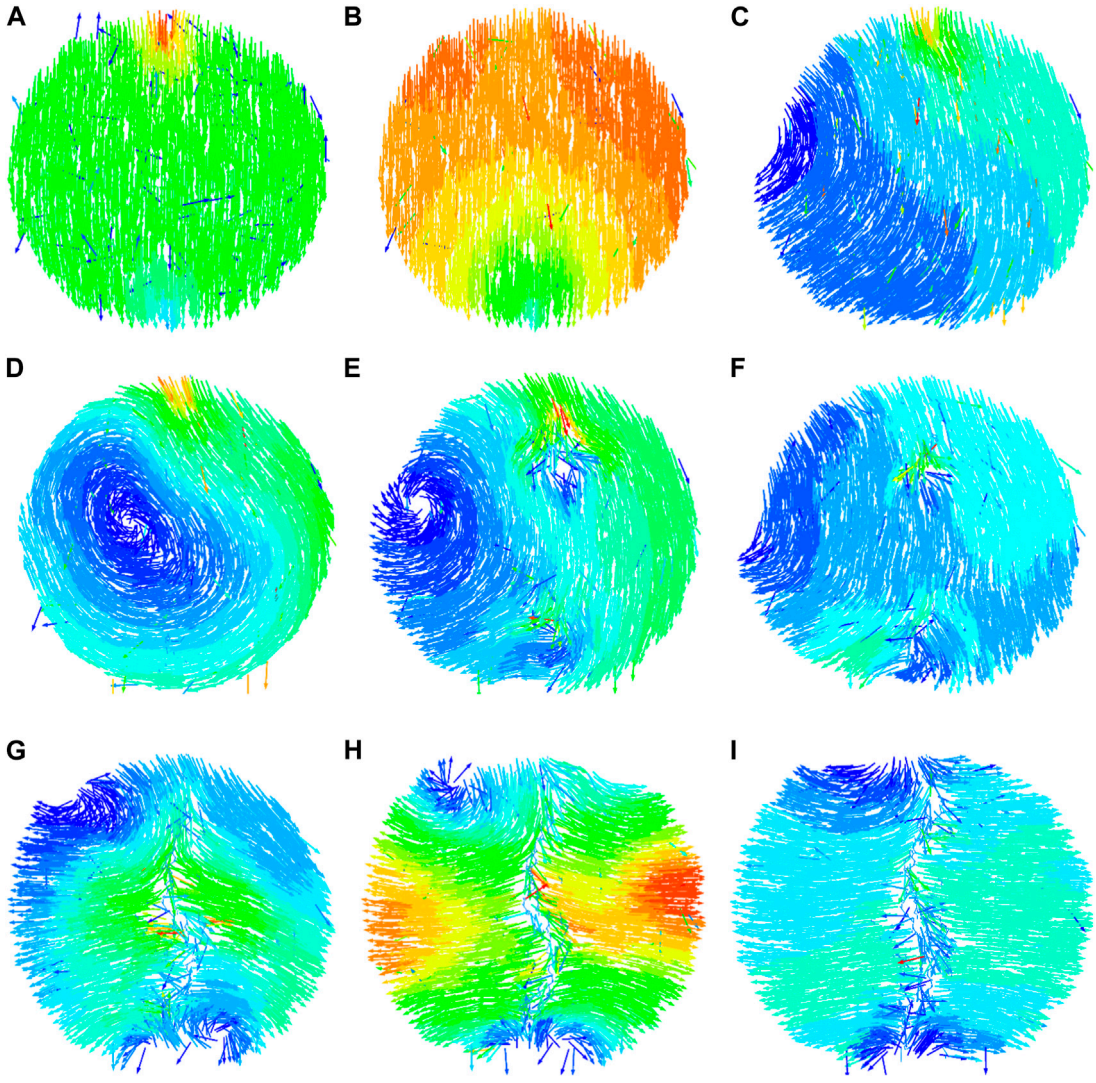

FIGURE 12
Nephogram of aggregate displacement during compression to damage. [The letters **(A–I)** indicate different compression stages, from the initial state to the final failure state, arranged in chronological order].

mechanisms and influential factors of geopolymers on cold mixes, thus providing a new tool and basis for evaluating and improving the strength and water stability of cold mixes.

5 Conclusion

Distinguished from previous investigations, the current work sought to systematically assess the impacts of geopolymer modification on the performance of cold mixed asphalt, while elucidating the underpinning mechanisms to provide guidance on mix design and formulation. Fluorescence microscopy and discrete element modeling were engaged to probe the microstructure and compressive behavior of the cold mix, thereby revealing the action mechanism and influencing factors of the geopolymer on the cold mix more comprehensively. Rather than examining individual parameters, this study incorporated various factors impacting the strength and water stability of cold mixes, encompassing the geopolymer dosage, immersion conditions, and curing duration, thereby enhancing the applicability and significance of the study outcomes in a more accurately way. The main results are summarized as follows.

(1) With incremental geopolymer additive content, the stability of the cold mix initially accreted then waned, attaining its apex when the mass ratio between the base asphalt and geopolymer additive was 4:3.
(2) Temperature was the predominant factor impinging cold mix stability, while geopolymer incorporation did not effectively mitigate the temperature impacts on strength. As geopolymer additive increased, the residual stability declined progressively. The water damage resistance of the geopolymer was relatively feeble, and immersion at higher temperatures and longer durations engendered inferior cold mix strength and water stability.
(3) Analyzing the stability test outcomes at disparate curing ages elicited that cold mix strength enhanced with prolonged curing, albeit with attenuating strength growth rates. In conjunction with engineering requisites, curing durations no less than 3 days were recommended.
(4) Fluorescence microscopy of the cold mix discerned the asphalt enswathed by the gelated geopolymer products, thereby adhering to the aggregate surfaces to constitute strength. Discrete element simulations of Marshall stability tests further evinced the vertical orientation below the loading point endured the principal loading. The gelated geopolymer envelopment resisted vertical loading and substantially augmented the strength and stiffness of the cold mix.

While providing meaningful insights, certain limitations inherent in this study warrant further investigation. Firstly, quality control and specification standards of the geopolymer additives necessitate additional refinement and formulation. Moreover, continued efforts are necessary to optimize and evaluate the long-term performance, aging mechanisms, and water damage resistance of cold mixed asphalt. Furthermore, additional analysis and modeling of the stress-strain behavior, fatigue crack propagation, and damage evolution under diverse loading magnitudes, thermal conditions, and humidity environments remain imperative.

In summation, this study conducted systematic evaluation of the impacts of geopolymer modification on cold mixed asphalt performance, while elucidating the underpinning mechanisms to provide practical guidance on mix design and optimization. The pragmatic implications of the research findings will enable engineers to select suitable geopolymer additives and curing durations for engendering high-performance cold mix asphalt, thereby conferring economic, efficiency, and environmental benefits.

Data availability statement

The original contributions presented in the study are included in the article/Supplementary material, further inquiries can be directed to the corresponding author.

Author contributions

JF: Conceptualization, Methodology, Writing–original draft. HL: Data curation, Validation, Writing–review and editing. ZS: Conceptualization, Formal Analysis, Writing–review and editing. ZC: Conceptualization, Formal Analysis, Writing–review and editing.

Funding

The author(s) declare that no financial support was received for the research, authorship, and/or publication of this article.

Conflict of interest

Authors JF and ZS were employed by Shandong Hi-speed Construction Management Group Co., Ltd. Author ZC was employed by Shandong Expressway Peninsula Investment Co., Ltd.

The remaining author declares that the research was conducted in the absence of any commercial or financial relationships that could be construed as a potential conflict of interest.

Publisher's note

References

Alnadish, A. M., Singh, N. S. S., and Alawag, A. M. (2023). Applications of synthetic, natural, and waste fibers in asphalt mixtures: a citation-based review. *Polymers* 15 (4), 1004. doi:10.3390/polym15041004

Andrews, J. K., Radhakrishnan, V., Koshy, R. Z., and Prasad, C. S. R. K. (2023). Construction and evaluation of low-volume roads incorporating emulsion treated base layers. *Indian Geotechnical J.* 53, 1041–1052. doi:10.1007/s40098-023-00724-5

Bi, Y., Li, R., Han, S., Pei, J., and Zhang, J. (2020). Development and performance evaluation of cold-patching materials using waterborne epoxy-emulsified asphalt mixtures. *Materials* 13 (5), 1224. doi:10.3390/ma13051224

Cai, X., Huang, W., Liang, J., and Wu, K. (2020). Study of pavement performance of thin-coat waterborne epoxy emulsified asphalt mixture. *Front. Mater.* 7, 88. doi:10.3389/fmats.2020.00088

Deb, P., and Singh, K. L. (2022). Mix design, durability and strength enhancement of cold mix asphalt: a state-of-the-art review. *Innov. Infrastruct. Solutions* 7 (1), 61. doi:10.1007/s41062-021-00600-2

Deb, P., and Singh, K. L. (2023). Experimental investigation on the mechanical performance of cold mix asphalt using construction demolition waste as filler. *Int. J. Pavement Res. Technol.* 16, 1618–1635. doi:10.1007/s42947-022-00216-4

Dulaimi, A., Qaidi, S., Al-Busaltan, S., Milad, A., Sadique, M., Kadhim, M. A., et al. (2023). Application of paper sludge ash and incinerated sewage ash in emulsified asphalt cold mixtures. *Front. Mater.* 9. doi:10.3389/fmats.2022.1074738

Duxson, P., Fernández-Jiménez, A., Provis, J. L., Lukey, G. C., Palomo, A., and van Deventer, J. S. J. (2007). Geopolymer technology: the current state of the art. *J. Mater. Sci.* 42, 2917–2933. doi:10.1007/s10853-006-0637-z

Guo, M., Liang, M., Liu, H., and Du, X. (2023). Optimization and validation of waste bio-oil based high-performance rejuvenator for rejuvenating aged bitumen. *Mater. Struct.* 56, 99. doi:10.1617/s11527-023-02189-7

Hamid, A., Alfaidi, H., Baaj, H., and El-Hakim, M. (2020). Evaluating fly ash-based geopolymers as a modifier for asphalt binders. *Adv. Mater. Sci. Eng.* 2020, 1–11. doi:10.1155/2020/2398693

Jindal, B. B., Alomayri, T., Hasan, A., and Kaze, C. R. (2023). Geopolymer concrete with metakaolin for sustainability: a comprehensive review on raw material's properties synthesis performance and potential application. *Environ. Sci. Pollut. Res.* 30, 25299–25324. doi:10.1007/s11356-021-17849-w

Liu, Y., and You, Z. P. (2011). Accelerated discrete-element modeling of asphalt-based materials with the frequency-temperature superposition principle. *J. Eng. Mech.* 137 (5), 355–365. doi:10.1061/(asce)em.1943-7889.0000234

Meocci, M., Grilli, A., LaTorrte, F., and Bocci, M. (2017). Evaluation of mechanical performance of cement-bitumen-treated materials through laboratory and *in situ* testing. *Road Mater. Pavement Des.* 18 (2), 376–389. doi:10.1080/14680629.2016.1213506

Ministry of Transport of the People's Republic of China, (2004). *Technical specifications for construction of Highway asphalt pavements (JTG F40-2004)*. Beijing, China: China Communications Press.

Mirabdolazimi, S. M., Pakenari, M. M., and Kargari, A. (2021). Effect of nanosilica on moisture susceptibility of asphalt emulsion mixture. *Arabian J. Sci. Eng.* 46, 11139–11151. doi:10.1007/s13369-021-05696-3

Mondal, A., Ransinchung, R. N. G. D., and Choudhary, J. (2023). Sustainable recycling of industrial waste fillers and reclaimed asphalt pavement to produce environmentally feasible warm mix asphalt. *Innov. Infrastruct. Solutions* 8, 34. doi:10.1007/s41062-022-01006-4

Mostafa, A. E. A. (2015). Studying the Effect of using nano-materials on the performance of cold recycled asphalt pavement mixes. *Int. J. Adv. Eng. Technol.* 2 (11), 34–39.

Olsson, E., Jelagin, D., and Partl, M. N. (2019). New discrete element framework for modelling asphalt compaction. *Road Mater. Pavement Des.* 20, S604–S616. doi:10.1080/14680629.2019.1633750

Perca, L. A., Hashemian, L., Liu, J., et al. (2019). "Performance evaluation of fiber modified asphalt mixes in cold regions," in TAC-ITS Canada Joint Conference, Halifax, NS, June, 2019.

Provis, J. L., Duxson, P., Lukey, G. C., et al. (2006). Modeling the formation of geopolymers. *J. Am. Ceram. Soc.* 2006.

Wang, A. G., Zheng, Y., Zhang, Z. H., et al. (2019). Research progress of geopolymer cementitious material modification for improving durability of concrete. *Mater. Rep.* 33 (15), 2552–2560. doi:10.11896/cldb.19040211

Wang, Q., Kang, S. R., et al. (2020). Structural modeling and molecular dynamics simulation of geopolymers gel. *Mater. Rep.* 34 (4), 4056–4061. doi:10.11896/cldb.19030097

Wang, Y., Leng, Z., Li, X., and Hu, C. (2018). Cold recycling of reclaimed asphalt pavement towards improved engineering performance. *J. Clean. Prod.* 171, 1031–1038. doi:10.1016/j.jclepro.2017.10.132

Wielinski, J., Varamini, S., Esenwa, M., et al. (2019). "Design and field performance of cold-constructed asphalt pavements (CCAP) with gelled asphalts," in Proceedings of the 64th Annual Conference of the Canadian Technical Asphalt Association (CTAA), Halifax, Nova Scotia, November, 2019, 1–16.

Xiao, Y., Yunusa, M., Yan, B., Zhang, X., and Chang, X. (2021). Micro-morphologies of SBS modifier at mortar transition zone in asphalt mixture with thin sections and fluorescence analysis. *J. Infrastructure Preserv. Resil.* 2, 23. doi:10.1186/s43065-021-00037-y

Yang, X. (2019). *The research on preparation and properties of composite modified cold mix asphalt material*. PhD thesis. Dalian, China: Dalian University of Technology.

Yang, X. L., Li, B., and Li, X. H. (2014). Study on mechanical properties of cold mix asphalt mixture with fly ash. *J. China Foreign Highw.* 34 (4), 262–267. doi:10.14048/j.issn.1671-2579.2014.04.062

Yao, H., Xu, M., Liu, J., Liu, Y., Ji, J., and You, Z. (2022). Literature review on the discrete element method in asphalt mixtures. *Front. Mater.* 9. doi:10.3389/fmats.2022.879245

Zhang, T. (2007). *Research on cold mix and cold laid mixture*. PhD thesis. Chongqing, China: Chongqing University.